Segmentation of combinations of mean diffusivity and DCE perfusion derived CBV in Glioblastoma multiforme

R. Awasthi[1], R. K. Rathore[2], J. K. Singh[2], N. Husain[3], P. Soni[3], R. K. Singh[4], S. Behari[4], R. K. Gupta[1], and S. Kumar[5]

[1]Radiodiagnosis, Sanjay Gandhi Post Graduate Institute of Medical Sciences, Lucknow, India, Lucknow, Uttar Pradesh, India, [2]Mathematics & Statistics, Indian Institute of Technology, Kanpur, Kanpur, Uttar Pradesh, India, [3]Pathology, Chatrapati Sahu ji Maharaj Medical University, Lucknow, Uttar Pradesh, India, [4]Neurosurgery, Sanjay Gandhi Post Graduate Institute of Medical Sciences, Lucknow, India, Lucknow, Uttar Pradesh, India, [5]Radiotherapy, Sanjay Gandhi Post Graduate Institute of Medical Sciences, Lucknow, India, Lucknow, India

Introduction

High grade brain tumors show heterogeneity in terms of varying cellularity and polymorphism[1,2]. Diffusion imaging, MR spectroscopy and perfusion MRI have been used in the evaluation of tumor heterogeneity. Dynamic contrast enhanced (DCE) derived cerebral blood volume (CBV) and Diffusion tensor imaging (DTI) derived mean diffusivity (MD) may relate to tumor necrosis/hypoxia and neovascularization; however the relationship between MD and CBV with respect to various tissue components of brain tumors is not yet completely evaluated.

Glioblastoma multiforme (GBM) is the most aggressive among gliomas and has hypoxic, cellular and necrotic regions. The prior knowledge in differentiating various tissue components is likely to be useful in terms of treatment planning of these patients. MD has previously been used to quantify cellularity and necrosis in brain tumors while CBV had been shown to correlate with neoangiogenesis[3]. However, in isolation none of these differentiates various tumoral components especially the hypoxic regions. Vascular endothelial growth factor (VEGF) is a marker of neoangiogenesis and CBV has shown to be its surrogate marker[4]. Hypoxia inducible factor (HIF)-1α is known to express in hypoxic regions that usually present in the vicinity of necrosis in the tumoral tissue. We hypothesize that if we combine MD and CBV together then their combination could differentiate hypoxic, cellular and necrotic components in GBM.

Materials and methods

***Subjects*:** Forty four previously untreated patients with a post operatively confirmed diagnosis of GBM were included in this study.

***Data acquisition*:** All patients underwent preoperative imaging with both conventional, DTI and DCE-MRI on a 1.5 Tesla scanner (Echo-speed plus, General Electric, Milwaukee, USA) using a quadrature transmit–receive head coil. Institutional ethics and research committee approvals were obtained. DTI was acquired by using a single-shot echo planar dual spin-echo sequence with ramp sampling. The b-factor was set to 0 and 1000 s/mm^2; TR=8s; TE=100ms; and NEX=8. Total 23 axial sections were acquired with a slice thickness of 3mm, with zero spacing, FOV of 240mm. DCE-MRI was performed using a three dimensional spoiled gradient recalled echo (3D-SPGR) sequence [TR/TE/flip angle/ number of excitation(NEX)/slice thickness/field of view (FOV)/matrix size=5.0ms/1.4ms/15º/0.5/6mm/360×270mm/128×128mm, number of phases=32]. At the fourth acquisition, Gd-DTPA-BMA (Omniscan, GE Healthcare, USA) was administered intravenously with the help of a power injector (Optistar^{TM} MR, Mallinckrodt, Liebel-Flarsheim, Ohio) at a rate of 5ml/sec, followed by a bolus injection of 30ml saline flush. A series of 384 images in 32 time points for 12 slices having the same location as that of DTI slices, were acquired with a temporal resolution approximately of 5.25sec. Prior to 3D SPGR, fast spin echo (FSE) T_1-weighted (TR/TE/NEX/slice thickness/FOV/matrix size= 375ms/9.4ms/1/6mm/360×270mm/256×256mm) and fast double spin echo PD and T_2 weighted (TR/TE1/TE2/NEX/slice thickness/FOV/matrix size= 3500ms/25ms/85ms/1/6/360×270mm/256×256mm) imaging were performed for the same slice position to quantify voxel wise pre-contrast tissue T10[4].

***MRI data processing and quantitative analysis*:** Voxel wise tissue T_{10} was calculated from FSE T_1, T_2 and PD weighted images. Corrected CBV maps were generated by removing the leakage effect of the disrupted BBB[4]. For the calculation of perfusion metrics, a quantitative analysis of the concentration time curve was performed for calculation of cerebral blood volume (CBV). The segmentation methodology used a two layer generalized learning vector quantization (GLVQ) classification network[5].Here we have used CBV and MD maps (Fig.1 c&d) as an input feature vector for GLVQ clustering networks. Since both the maps (CBV and MD) have different range of data values, first we normalize these maps in same data range, which was [0, 255] in our case. Prototypes or weight vectors were initialized by making random draws from uniform distribution on [0, 255] for each coordinate of each prototype. Termination threshold ε = 0.5 is used as stopping criterion. Maximum number of iterations used as 10000. By using these input parameters brain tumor was classified in to four regions, which were in combination of high CBV-high MD (hh), high CBV-low MD (hl), low CBV-high MD (lh) and low CBV-low MD (ll). The mean values obtained from these segmented regions were used for the statistical analysis. Relative quantification of CBV (rCBV) was performed by placing the ROI on normal contra-lateral grey/white matter of the brain.

Histopathology*:* The excised GBMs were immuno-stained for monoclonal antibody against human hypoxia inducible factor (HIF)-1α (2C3, sc-21733, CA) and vascular endothelial growth factor (VEGF) (A-20) antigen. Each immunostained slide was digitized with 10X objective using Canon Power Shot G5 camera and the captured images were subjected to morphometry analysis. The percentage of ten areas with maximal positive staining was calculated at 10X resolution.

***Statistical analysis*:** Mean values of different combinations of MD and CBV were obtained by using descriptive statistics.

Results: We were able to segment the tumor tissue using CBV and MD maps (Fig 1e), and from the segmented regions we found four combinations of CBV and MD values. Mean values of MD (in 10^{-3}mm^{2}sec^{-1}) and CBV (in ml/100gm) with a) high rCBV-high MD were 3.93±1.84 & 1.26±0.19 b) high rCBV-low MD were 4.02±1.96 & 0.70±0.06, c) low rCBV-high MD were 0.85±0.45 & 1.42±0.28 and d) low rCBV-low MD were 1.0±0.40 & 0.70±0.07

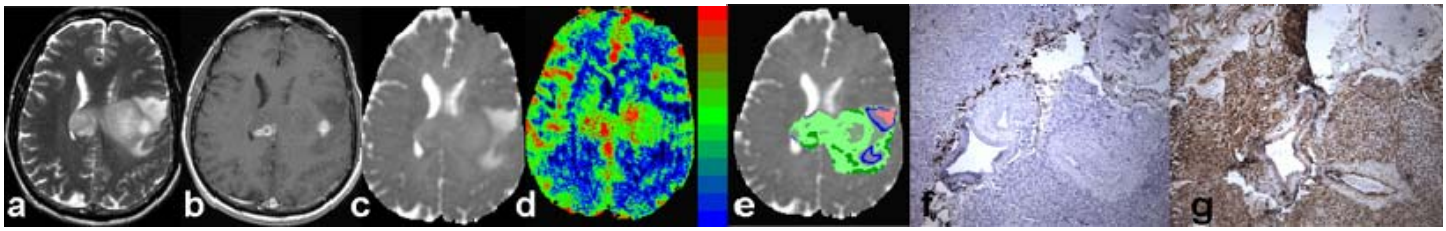

Fig1. a-e; T2, Post contrast T1, MD, RGB-CBV map, Segmented color map of tumor tissue overlaid on MD in which pink representing regions with high MD and low Perfusion, blue as both MD and perfusion low, grey with both MD and Perfusion high and green as high perfusion and low MD; Immunohistochemical expression of [f] HIF-1 α and [g] VEGF

On immunohistochemistry, HIF-1α was found to be expressed in the regions bordering necrosis while VEGF showed more uniform and broad expression throughout the tumoral tissue (Fig.1 f&g).

Discussion: In this study we have found that the four different combinations of MD and CBV values obtained after segmentation of the tumoral tissue can be used to differentiate hypoxic necrotic and well perfused tissues. We hypothesize that the regions with low MD and low perfusion represents the hypoxic areas, with low perfusion and high MD indicate necrotic tissue, with high perfusion and low MD represent the well perfused-high cellular tumor. The regions of tumor with both perfusion and MD high may be explained as the regions which are well perfused-cellular areas with increased intercellular spaces. Our hypothesis is supported by the degree and pattern of immunohistochemical expression of HIF-1 α and VEGF in these tumors tissues. We conclude that segmentation based on both CBV and MD may potentially allow for differential dose distribution using intensity modulated radiotherapy approaches and concurrent chemotherapy for GBM.

References

1.Cha et al. *AJNR Am J Neuroradio*2006;27:475–487, 2.De Angelis et al. *N Engl J Med* 2001;344:114–123, 3. Price J. *Br J Neurosurg.* 2007;21(6):562-75, 4. Haris M. *J Comput Assist Tomogr.* 2008;32(6):955-65, 5.Pal et al. *IEEE Trans. Neural Networks* 1993;4:549-558,